Image Cover Sheet

CLASSIFICATION	SYSTEM NUMBER
UNCLASSIFIED	150051

TITLE

INFRARED AND MILLIMETER WAVE DETECTION USING THIN FILMS OF PB DOPED BiSrCaCuO SUPERCONDUCTORS

System Number:

Patron Number:

Requester:

Notes:

DSIS Use only:

Deliver to: NL

Infrared and millimeter wave detection using thin films of Pb doped BiSrCaCuO superconductor

L. Ngo Phong
Defence Research Establishment Valcartier
P.O. Box 8800, Courcelette, QC G0A 1R0, Canada

#150051

ABSTRACT

Thin film detectors made of CuO superconductors were developed in our laboratory. This article reports details of the fabrication and testing of Pb doped BiSrCaCuO detectors. The detector comprises a film sensor housed in a small cryostat with built-in bias supply and temperature control circuitry. The film sensor was first deposited by magnetron rf sputtering and then crystallized under a rapid thermal annealing process. The characteristics of the response of the detector under millimeter wave and infrared illumination were investigated. The millimeter wave response exhibited a Josephson component with a $D^* \sim 10^8 - 10^9$ cm.Hz$^{1/2}$/W in the wavelength range of 3 - 8 mm. The transient response to short pulses indicated a time constant $\tau \leq 10$ ns for this component. The response to laser pulses was thermal in origin and inherently compressible, preventing saturation of the detector electronics to intense beams. The wide band characteristic of the responses at both infrared and millimeter wavelengths could be confirmed. The damage threshold of the film sensor was shown to exceed 10 mJ / cm^2 per 3 ns pulse. The possible use of these detectors for threat detection and the optimization of their figure of merit are discussed.

I. INTRODUCTION

The worldwide arsenal of radar- and laser-aided weapons is growing in numbers and sophistication. The recent advances in tunable sources with sufficiently high power densities led to the requirement for an extended band width of future threat classification and localization devices. A solution to increasing the effective wavelength band of the latter devices is to combine the use of different detectors. In general, these detectors have dissimilar properties and operating requirements so that the design of a hybrid device may be complex. The use of a single wide band detector offers a simpler alternative. Furthermore, it is better suited to certain configuration designs for wavelength discrimination or direction finding. The efficiency of conventional wide band detectors, however, is limited either by their low speed and detectivity or by the liquid helium cooling requirement.

Superconductors can be used as wide band detectors under specific conditions. Fast sensitive responses have been demonstrated at infrared and millimeter wavelengths in thin films of low temperature BaPbBiO and Sn.[1,2] The sensing applications of the recent CuO superconductors with critical temperatures (T_c) above 77 K have, therefore, received considerable attention. In this work, the fabrication and testing of Pb doped BiSrCaCuO thin film detectors were specifically investigated. The relevant details of the device fabrication are described in section II. In sections III and IV the characteristics of the responses at infrared and millimeter wavelengths are presented and discussed. The main focus in the discussion of the results is on the identification of the detection modes from the response signatures.

II. DEVICE FABRICATION

The enhanced formation of the high T_c $Bi_2Sr_2Ca_2Cu_3O_{10}$ phase by the addition of lead was confirmed in our previous work.[3] To fabricate the sensing device with a high operating temperature, single target magnetron rf sputtering has first been used to deposit Pb doped BiSrCaCuO onto (100) $LaAlO_3$ or MgO substrates. The sputter target was manufactured under a solid state reaction of high

Paper presented at the Mission Systems Panel 1st Symposium on "Guidance and Control for Future Air-Defence Systems" held in Copenhagen, Denmark from 17th May to 20th May 1994.

purity compounds of PbO, Bi_2O_3, $SrCO_3$, $CaCO_3$, and CuO. The stoichiometric weight of each compound j was

$$M_j = n_j \mu_j M_t / \Sigma (n_j \mu_j), \quad (1)$$

where n_j is the number of moles required for achieving the nominal composition Pb:Bi:Sr:Ca:Cu = 2:2:2:2:3 of the target, μ_j is the molecular weight, and M_t, 35 g, is the weight selected for the target. These compounds were repeatedly mixed, ground, and sintered during 12 hours at 800 °C in air. The resulting homogeneous, well-reacted mixture was pressed at 140 MPa into a disk target with a diameter of 50 mm. The disk target was subsequently bonded to a copper base plate using silver epoxy. The copper plate served as a mechanical support and provided a better thermal conductivity between the target and the heat sink.

The rf sputtering deposition was performed in 4 mTorr of argon at a power level of 80 W. The distance between the target and the substrate table was 8 cm. The thickness and area of the substrate were respectively 200 μm and 1 cm^2. The substrates were mounted on the substrate table at a distance from 3 to 4.5 cm with respect to the discharge axis. In this range the deposition rate was established to be ~ 10 nm/min. The deposition time was controlled to produce films with thicknesses ranging from 200 to 1000 nm. The as-deposited films were amorphous and insulating as no intentional heating was applied to the substrates during the deposition. A short thermal annealing, first in oxygen and then in air, was necessary to form the superconducting phases. The temperature for annealing in oxygen ranged from 810 to 830 °C, and that in air from 830 to 870 °C. The annealing times were varied for different samples, with maxima of 20 and 40 min in oxygen and air respectively. The effects of annealing parameters on the film properties have been reported elsewhere.[4] In this work, mainly granular films of $Bi_2Sr_2CaCu_2O_8$ - $Bi_2Sr_2Ca_2Cu_3O_{10}$ multiphase were used since the Josephson detection was of primary interest. These films show typically a sheet resistance R_s ~ 24 Ω / □ at 300 K and a resistance transition in the vicinity of 100 K.

The film sensors were patterned into meander line

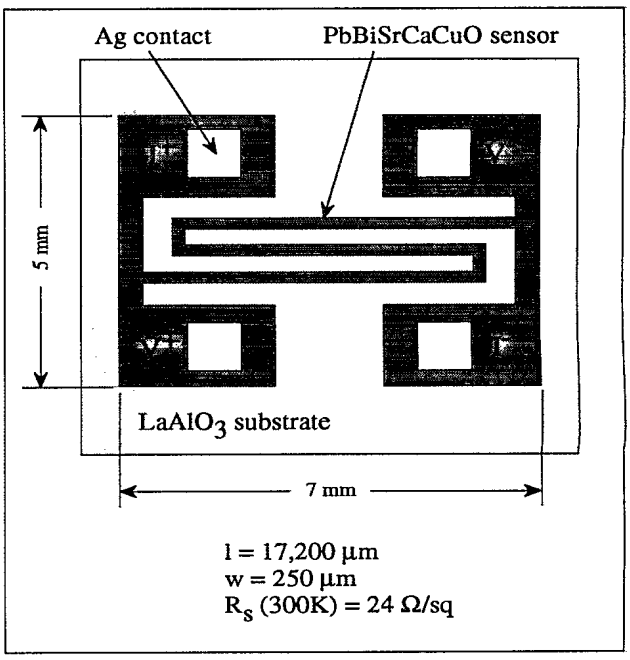

FIG. 1. PbBiSrCaCuO meander line sensor in four-terminal configuration.

structure with a length-to-width ratio l / w ~ 70. The patterning process was performed by first coating a 1-μm thick layer of positive photoresist onto the superconductor film. The film with the coated photoresist was exposed under ultra violet light for about 40 s with a photomask placed directly on it. The photoresist was subsequently developed in a solution for about 2 min and washed in de-ionized water. To remove the unwanted film areas, the sample was immersed in diluted HCl at room temperature for a period of about 10 s. After the etching, the sample was immersed in acetone to remove the photoresist on the superconductor pattern. Once done, an Al mask was placed in direct contact to the film with the four square windows aligned to the four rectangular contact pads in the pattern. The electric contacts to the sensor were formed by vacuum evaporation of Ag. The resulting superconductor sensor is schematically shown in Fig. 1.

In order to construct the detector unit, the sensor was thermally anchored to the cold finger of a small liquid nitrogen cryostat with photon access via a ZnSe window. The infrared and millimeter wavelength transmittances of this window were measured to be ~

0.9 and 0.7 respectively. The sensor temperature was first monitored by a Si sensor imbedded in the cold finger and then relayed to a feedback controller circuit. This circuit set the sensor temperature to the desired value by adjusting the thermal load of 2 high power transistors located on both sides of the sensor. The built-in bias supply consisted of standard 3 V lithium cells providing dc currents of up to 20 mA in the sensor through a variable resistor. The voltage signal generated across the sensor was driven to an rf amplifier with a band width of ~ 500 MHz and a gain of ~ 30 dB. All detectors have a bnc output connector and are terminated into 50 Ω. A 500 MHz digitizing oscilloscope with a resolution of 500 ps was used to record the voltage signals. A lock-in amplifier was occasionally used to detect the rms voltage fluctuation under modulated cw illumination or dark condition (noise). The voltage sensitivity of the lock-in amplifier was set at 0.1 nV for a frequency of 5 kHz. For the purpose of recording the resistance-temperature characteristics of the detector, a nanovoltmeter was also used to measure the output dc voltage.

III. MM-WAVE DETECTION

The millimeter wave was generated by different Gunn diode oscillators operating in the frequency band from 35 to 90 GHz (λ = 8.6 to 3.3 mm). The maximum cw power P_T of this source was measured to be ~ 70 mW. The main component of the millimeter wave was transmitted to the superconductor detector from a pyramidal horn antenna. The gain of the antenna of height H and width W was estimated as

$$G_T(\lambda) = 4\,\varepsilon\,\pi\,H\,W\,/\,\lambda^2, \qquad (2)$$

assuming an aperture efficiency $\varepsilon \approx 50$ %. Typically, G_T is ~ 25 dB at λ = 8.6 mm. With the far field condition $z > 2\,W^2 / \lambda$ satisfied, the power density p of the radiation incident on the detector could be evaluated,

$$p(\lambda) = P_T\,G_T\,\eta\,/\,4\,\pi\,z^2, \qquad (3)$$

where z is the separation between the antenna and the detector, and η denotes the transmittance of the ZnSe window at wavelength λ. The millimeter wave source could be operated either in cw or pulsed mode. In cw operation mode the incident radiation was amplitude modulated into square wave pulses with a 50% duty cycle. This was done by using a wave form generator which drives the electronics control of the Gunn diode. The pulse at this generator was further relayed to the lock-in amplifier so that the modulation frequency f served as a reference frequency in the detection. In pulsed operation mode the pulse at the wave form generator was transmitted to a broadband p-i-n switch in the waveguide through a driver. The p-i-n device provided a relatively fast switching of the incident wave so that pulses with a width as narrow as 30 ns could be produced. To characterize the transient power of the incident wave, a portion of it was driven to a fast GaAs point contact detector via a directional coupler.

It was previously established [5] that the interaction between millimeter wave photons and superconductors may lead to two principal response modes, hereby referred to as bolometric and nonbolometric modes. In the bolometric mode, radiation induces a temperature rise δT in the superconductor film sensor by lattice heating. When the sensor is current biased at a given temperature in the resistance transition region, this results in an increase δR of the bias resistance which produces a voltage change δV across the sensor. If δT is small compared to the transition width, then the responsivity r of a sensor with an active area S can be expressed as

$$r = I\,\delta R\,/\,\alpha\,p\,S \approx I\,(\partial R/\partial T)\,\delta T\,/\,\alpha\,p\,l\,w, \qquad (4)$$

where I is the dc bias current and α is the power absorbance. This equation provides insight as to the specific behavior of the bolometric responsivity. It suggests, for instance, that the temperature dependence of r is similar to that of $\partial R\,/\,\partial T$, provided that any variation of δT and α in the temperature range considered can be neglected. A deviation from this behavior may be indicative of a nonbolometric mechanism such as the Josephson detection. However, no conclusion can be drawn from this criterion alone.

To envision the effect of operating temperature, in Fig. 2 the responsivity r of a representative detector to

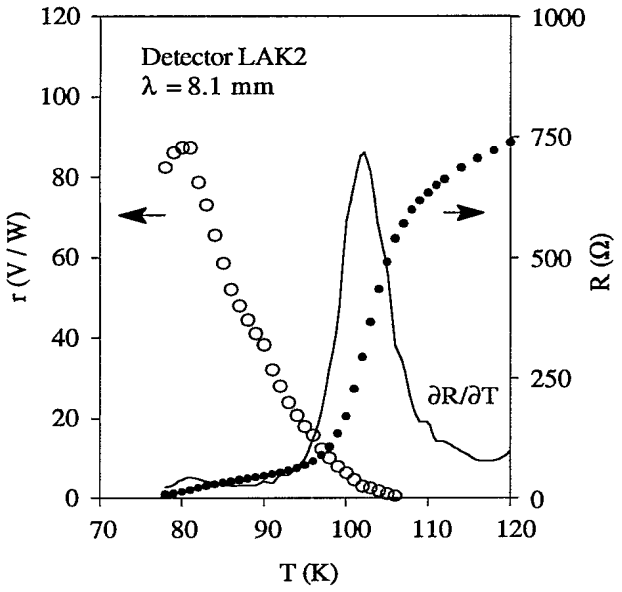

FIG. 2. Left vertical scale (open circles): temperature dependence of the mm-wave responsivity, I = 2.5 mA, f = 100 Hz. Right vertical scale (solid dots): resistance-temperature characteristic of the detector measured at I = 2.5 mA. The solid line shows the temperature variation of ∂R/∂T.

modulated 8.1-mm cw radiation is plotted versus T. Here, r denotes the rms value of δV normalized to the cw power delivered onto the sensor assuming $\alpha = 1$. The detector was biased at I = 2.5 mA. Its R - T characteristic at the same magnitude of I and the corresponding temperature dependence of $\partial R / \partial T$ are also shown. We noted that the superconductor sensor exhibits a T_{onset} ~ 110 K and a T_c ~ 77 K, which are indicative of the constituent $Bi_2Sr_2CaCu_2O_8$ - $Bi_2Sr_2Ca_2Cu_3O_{10}$ multiphase. This rather broad transition suggests also a strong granularity of the device. As the sensor is first biased into a partially resistive regime where $\partial R / \partial T$ values are small, r is seen to reach a peak value at T = 80 K. With T increasing further to about 106 K at which $\partial R / \partial T$ peaks, r decreases by contrast to the noise level. It appears from this discrepancy that the behavior of r (T) deviates from that predicted by the thermal model. Further disagreement with the thermal model stems from the fact that the responsivity of ~ 90 V / W measured at T = 80 K is many times larger than the largest possible value of bolometric responsivity. In effect, the upper bound on the bolometric responsivity could be estimated as follows. After a haft cycle period $t = 1 / 2f$ the maximum heat energy received by the sensor is $\in = p / 2f$, assuming full absorption and neglecting any cooling. The temperature increase due to heat storage within a diffusion length $\xi \approx (Dt)^{1/2}$ in the sensor of specific heat c and thermal diffusivity D is

$$\delta T = \in / c\,\xi = (p / c)\,(t / D)^{1/2}. \qquad (5)$$

To evaluate more precisely δT we need to compare the thermal diffusion length ξ to the sensor thickness υ. Using typical values of thermal conductivity[6] ($k \approx 10^{-2}$ W / cm K) and specific heat[7] ($c \approx 0.9$ J / cm^3 K) around T_c for BiSrCaCuO, the diffusivity constant was estimated to be $D \approx k / c = 1.1 \times 10^{-2}$ cm^2 / s. It follows that $\xi >> \upsilon$ for f = 100 Hz, where $\upsilon \approx 400$ nm. Since the absorbed heat was assumed to be confined in the sensor during the period t, the value of υ is taken for ξ_{max}. Therefore, according to Eqs. (4) and (5) the bolometric responsivity should not exceed

$$r_{max} \approx I\,(\partial R / \partial T) / 2f c\,\upsilon\, l\, w. \qquad (6)$$

Referring to Fig. 2, the magnitude of $\partial R / \partial T$ can be derived to be ~ 3.3 Ω / K at T = 80 K, yielding $r_{max} \approx$ 26 V / W. This value is seen to be much smaller than the measured responsivity despite the assumption that the heat energy was totally absorbed and confined in the sensor. Since a bolometric component may contribute negligibly to the overall response in the vicinity of T_c, this response is believed to be predominantly nonbolometric.

Further support to the nonbolometric origin of the response stems from the observation that the rms value of δV remained unchanged as f was increased. Whereas the detector exhibits a square law response to low power radiation, that is, $\delta V \propto p$, the above observation clearly shows that δV is independent of heat energy delivered to the sensor. Moreover, the transient voltage response of the sensor was observed to reproduce the square wave pulse of the cw radiation, indicating that it has a short time constant. To confirm the high speed detection of the superconductor sensor, its response to short millimeter wave pulses was investigated. Figure 3 shows the transient voltages of both incident and detected signals

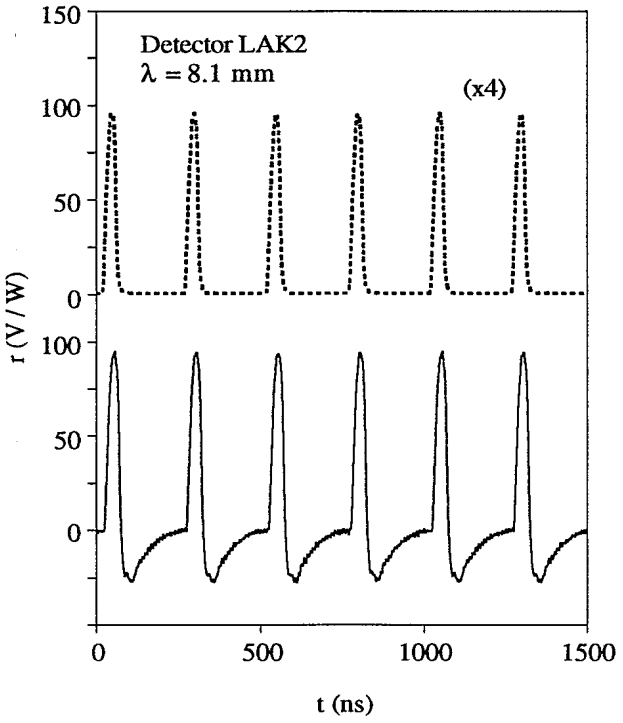

FIG. 3. Top (dotted line): incident millimeter wave pulses recorded by a GaAs point contact detector, the responsivity of which was magnified 4 times for comparison. Bottom (solid line): corresponding transient response of a PbBiSrCaCuO detector at T = 80 K and I = 1.5 mA.

as normalized to the peak power generating each signal. At a repetition frequency of 4 MHz, the incident pulses were recorded with a fast GaAs point contact detector and detected simultaneously with the PbBiSrCaCuO detector. The latter detector was biased at T = 80 K and I = 1.5 mA, where its responsivity is seen to be about 4 times larger than that of the GaAs detector. The rise time t_r, fall time t_f, and pulse width Δt of the incident and detected pulses are compared in Table I. It can be seen that, except for a small difference in pulse width, the temporal structure of the incident pulse could be reproduced with the superconductor detector. The response time τ of this device, defined as the recovery time of the response signal from 100 % to 36 % of its amplitude, was measured to be less than 10 ns. As compared to the diffusion time $t_d \sim \upsilon^2 / D$ for heat propagation through the film sensor along c-axis, τ is approximately 15 times shorter. Such a response speed is too fast to be consistently attributed to a thermal mechanism. Another

TABLE I. Time constants of incident and detected millimeter wave pulses. The incident pulses were characterized with a GaAs point contact detector and detected with a PbBiSrCaCuO detector operating at T = 80 K and I = 1.5 mA.

	Incident pulse	Detected pulse
$t_{r\ 10\%\text{-}90\%}$ (ns)	17.6	17.6
$t_{f\ 90\%\text{-}10\%}$ (ns)	11.2	11.2
$\Delta t_{\ 50\%}$ (ns)	31	33

feature that rules out this mechanism is the large responsivity of the detected signal. After a pulse period $t = \Delta t$ = 30 ns the thermal diffusion ξ can be estimated to be inferior to the sensor thickness υ. Combining Eqs. (4) and (5), the maximum bolometric responsivity

$$r_{max} \approx I\,(\partial R / \partial T)\,(t / D)^{1/2} / c\,l\,w, \qquad (7)$$

yields $r_{max} \sim$ 200 μV / W in this case. As anticipated from the short heating period, this value is excessively small compared to the detected signal amplitude. This observation, again, comfirms the occurrence of a nonbolometric detection mechanism under the conditions used in this study. Also noted in Fig. 3 is a secondary pulse component with reversed sign in the detected signal. Its origin has not been identified. Although the secondary pulse appears to have a large time constant, it also shows a large responsivity. The latter fact, in precise analogy to the above, excludes the bolometric mechanism as being responsible for the observed anomaly.

Since the observed nonbolometric response mode occurred solely in granular film sensors, the Josephson detection appears to be the most likely mechanism. A granular sensor may be modeled as an array of superconducting grains interconnected via Josephson junctions or weak links. This model assumes that the macroscopic response results from a superposition of the response signals of individual junctions forming the network. A discussion on this model has been given elsewhere.[5] In this work, we could further confirm the Josephson detection in the wavelength range from 3 to 9 mm. Figure 4 shows the wavelength dependence of the detectivity D^* of a PbBiSrCaCuO detector at T = 80 K and I = 2.5 mA. The detectivity

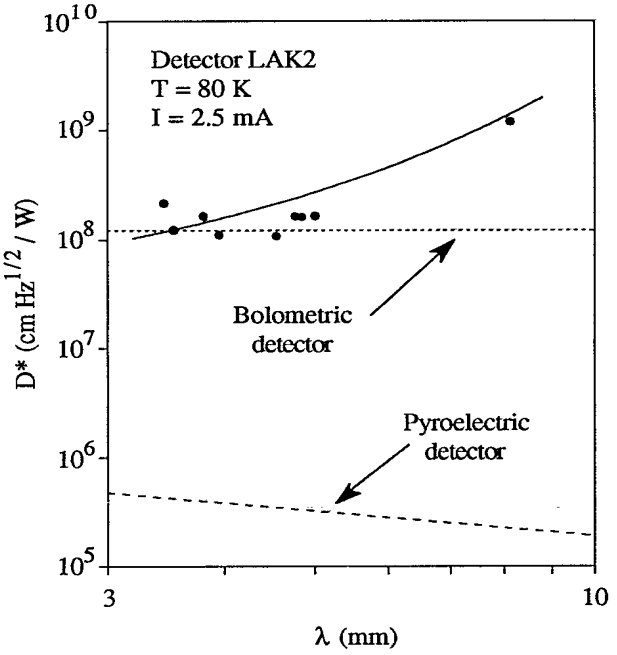

FIG. 4. Wavelength dependence of the detectivity of a PbBiSrCaCuO detector at f = 5 kHz. The solid line is provided as visual aid. The detectivities of a bolometric detector (S = 0.2 cm^2; τ = 35 μs; dotted line) and a pyroelectric detector (S = 0.03 cm^2; τ = 10 ms; dashed line) are also plotted for comparison.

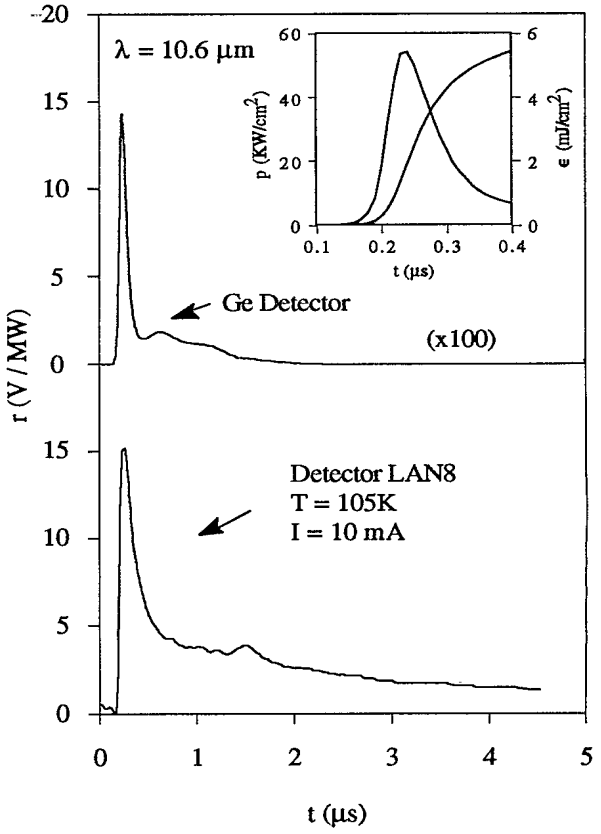

FIG. 5. Top: incident CO_2 laser pulse recorded by a Ge photon drag detector, the responsivity of which was magnified 100 times for comparison. Bottom: corresponding transient response of a PbBiSrCaCuO detector at T = 105 K and I = 10 mA. The inset figure shows the laser power density and fluence incident on the PbBiSrCaCuO detector on a smaller time scale.

was estimated from the noise measurement,

$$D^* = (S \Delta f)^{1/2} r / V_n , \qquad (8)$$

where $V_n \approx 20$ nV at f = 5 kHz and Δf = 2.45 Hz. Although the detector parameters and operating conditions have not yet been optimized, detectivities above 10^8 cm Hz$^{1/2}$ / W were obtained for λ in the range of 3 - 5 mm. At λ = 8.1 mm, the detectivity was evaluated to exceed 10^9 cm Hz$^{1/2}$ / W. These levels of D^* compare favorably with those of low speed, wide band detectors such as bolometric and pyroelectric [8] detectors. It should be recalled that the variation of α (λ) was not accounted for in the evaluation of r in Eq. (4). As a consequence of the assumption α = 1, the estimated values of D^* may be significantly smaller than the actual values. Furthermore, the wavelength dependence of the estimated D^* cannot be attributed to that of the Josephson responsivity alone. The increasing values of D^* at longer wavelengths appear, however, to be consistent with the λ^2 dependence of the Josephson responsivity. If this dependence holds for microwave frequencies, an increase of 1 - 2 orders of magnitude of D^* in this range may be anticipated.

IV. INFRARED DETECTION

As for millimeter wave photons, the interaction between infrared photons and superconductors may lead to a bolometric and a nonbolometric response mode. The bolometric mode results from the same temperature dependence of the sensor resistance as previously described. On the other hand, the mechanism of the infrared nonbolometric mode may differ from that responsible for the millimeter wave response. As the order parameter reported for $Bi_2Sr_2CaCu_2O_8$ films [9] is ~ 25 meV, infrared photons may cause dissociation of Cooper pairs and produce

TABLE II. Time constants of incident and detected CO_2 laser pulses. The incident pulses were characterized with a Ge photon drag detector and detected with a PbBiSrCaCuO detector operating at T = 105 K and I = 10 mA.

	Incident pulse	Detected pulse
$t_{r\,10\%\text{-}90\%}$ (ns)	40	41
$t_{f\,100\%\text{-}36\%}$ (ns)	70	250
$\Delta t_{50\%}$ (ns)	85	210

excess quasiparticles. Due to the resulting decrease of the relative fraction of Cooper pairs to quasiparticles, the Josephson critical current in the film is reduced. If the film is biased by a current close to the critical value, a fast voltage change will be induced under infrared illumination. In order to determine whether such a nonbolometric detection mode occurs in the fabricated detectors, their responses to short laser pulses were measured at different infrared wavelengths. The preliminary results of this study are described in this section.

In Fig. 5 the transient response of a PbBiSrCaCuO detector to 10.6-μm laser pulses is shown together with the laser pulse characteristic. The infrared source consisted of a TEA CO_2 pulsed laser with a beam diameter of about 2 mm at the output. A Ge photon drag detector was used to characterize the laser pulse. This detector has a responsivity of ~ 0.14 V / MW and a time constant smaller than 1 ns when terminated into 50 Ω. The power density p and fluence $\in$ of laser pulse incident on the superconductor sensor were measured to be about 54 kW / cm^2 and 15 mJ / cm^2 respectively. To facilitate the analysis of the result, the superconductor sensor was patterned into a bridge with an active area slightly larger than the beam size. The thickness of the sensor was 240 nm.

There are several features of the transient response of the PbBiSrCaCuO detector which suggest that it is rather predominantly thermal in origin. We first noted an increase of phase shift between the incident and detected signals, both of which simultaneously recorded, when the operating temperature T was decreased at temperatures below T_c. The observed time delay may correspond to the period of heat delivery required for increasing the sensor temperature from T

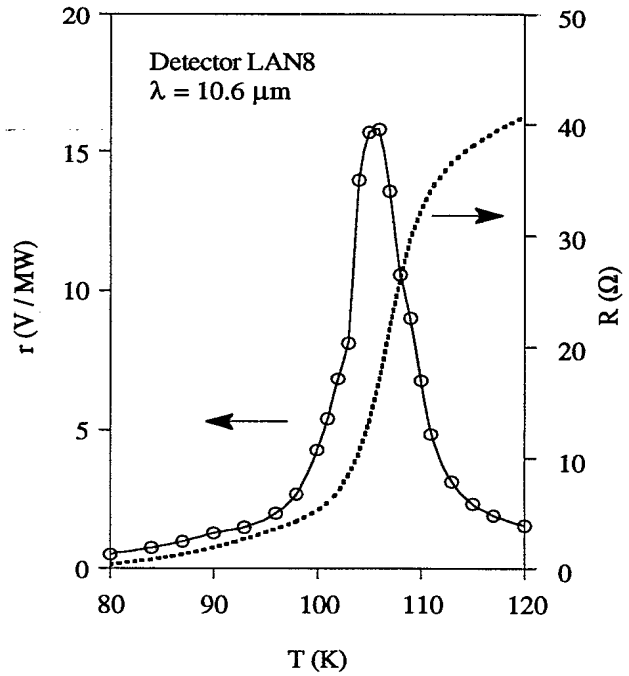

FIG. 6. Left vertical scale (open circles): temperature dependence of the responsivity to CO_2 laser pulses, I = 10 mA. Right vertical scale (solid dots): resistance-temperature characteristic of the detector measured at I = 10 mA. The solid line is provided as visual aid.

to ~ T_c where a response can be induced. Another relevant fact is the relatively slow recovery time of the transient response. Table II presents a comparison of the transient characteristics of the incident and detected pulses. Whereas the rise time remains unchanged for both pulses, the recovery time of the detected pulse is about 3.5 times larger than that of the incident pulse. Despite this difference, the time constants of the superconductor detector are seen to be small compared to those of conventional thermal detectors. This result may be partly attributed to the small thickness of the sensor.

Figure 6 illustrates the temperature dependence of the responsivity r and resistance R of the superconductor detector. Here, r denotes the peak voltage of the response signal, normalized to the peak power of the laser pulse incident on the sensor. Again, the behavior of r (T) is seen to be in good agreement with the thermal model described in Eq. (4) with δT ~ 0.7 K. At $T \approx$ 105 K where $\partial R / \partial T$ peaks, r also reaches its maximum value which, referring to Fig. 5, is about 2

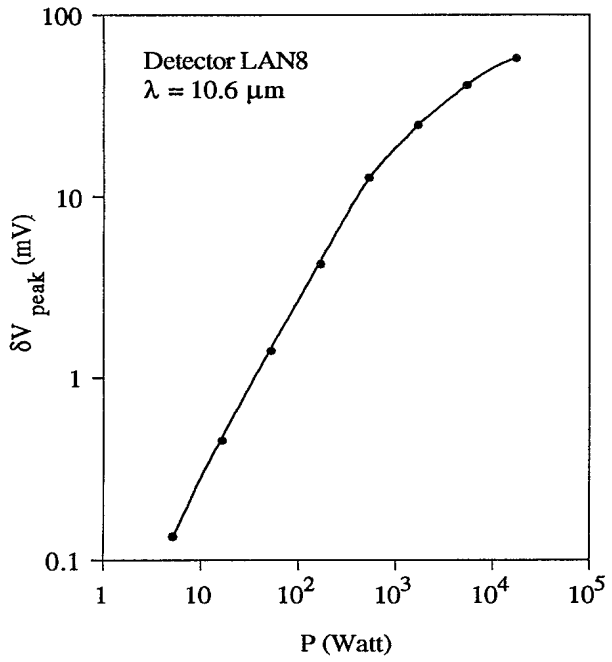

FIG. 7. Peak voltage response to CO_2 laser pulse as a function of laser power incident on the PbBiSrCaCuO detector, T = 105 K, I = 10 mA. The solid line is provided as visual aid.

orders of magnitude larger than the responsivity of the Ge detector.

As a direct result of its thermal origin, the infrared response of the superconductor detector is inherently compressible. This characteristic can be illustrated as follows. When the sensor is biased at an operating temperature T in the transition region, the voltage response can be expressed as

$$\delta V_1 (T) \approx I [R (T + \delta T) - R (T)]. \quad (9)$$

For simplicity, assuming that by doubling the power density p of the laser pulse the temperature increase δT attains twice its initial value, so that the voltage response becomes

$$\delta V_2 (T) \approx I [R (T + 2 \delta T) - R (T)]. \quad (10)$$

Referring to the R - T characteristic in Fig. 6, it can be seen that $\delta V_2 \approx 2 \delta V_1$ within the linear region of the transition, and $\delta V_2 < 2 \delta V_1$ when $T + 2 \delta T > T_{onset}$. It follows that, even if a linear relation between δT and p can be maintained, the one between δV

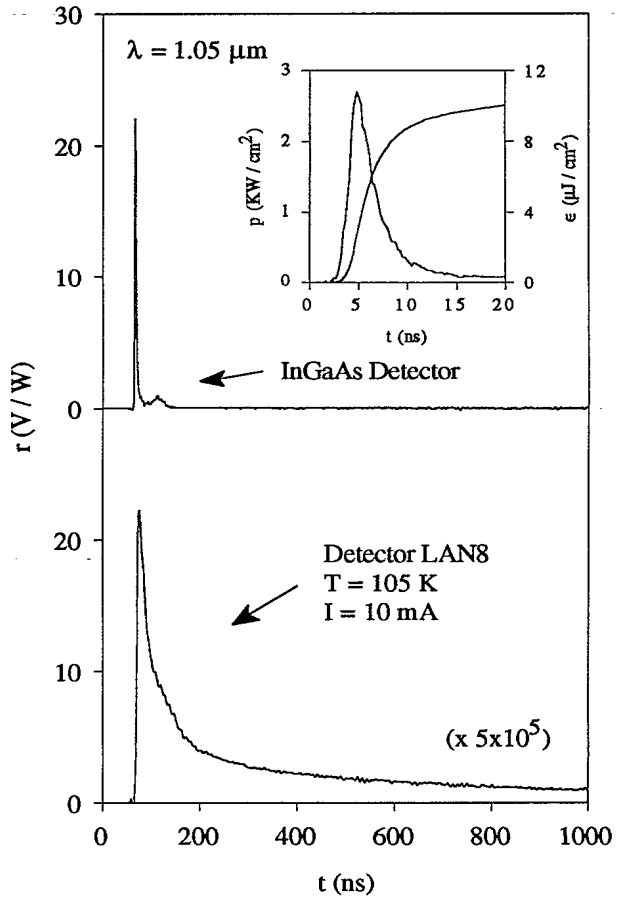

FIG. 8. Top: incident Q-switched Nd:YLF laser pulse recorded by an InGaAs detector. Bottom: corresponding transient response of a PbBiSrCaCuO detector at T = 105 K and I = 10 mA. The inset figure shows the laser power density and fluence incident on the PbBiSrCaCuO detector on a smaller time scale.

and p is nonlinear for large values of p. Figure 7 presents the power dependence of the voltage response of a superconductor detector operating at T = 105 K and I = 10 mA. As the laser power delivered to the sensor is increased by 10 dB, from 1.6 to 16 kW approximately, δV is seen to increase by only 3.6 dB. Such a compressible response makes it possible to prevent saturation of the detector electronics under illumination of high power lasers.

The characteristics of infrared detection given above could be further confirmed at shorter wavelengths. Figure 8 shows, for example, the transient response of the superconductor detector to 1.05-μm laser pulses, together with the laser pulse characteristic. The infra-

TABLE III. Time constants of incident and detected Nd:YLF laser pulses. The incident pulses were characterized with an InGaAs detector and detected with a PbBiSrCaCuO detector operating at T = 105 K and I = 10 mA.

	Incident pulse	Detected pulse
$t_{r\,10\%\text{-}90\%}$ (ns)	2	5
$t_{f\,100\%\text{-}36\%}$ (ns)	3	50
$\Delta t_{50\%}$ (ns)	3	28

red source consisted of a Q-switched Nd:YLF laser with a beam diameter of about 2.5 mm at the output. In order to characterize the laser pulse, an InGaAs detector with a response time of ~ 500 ps was used. The power density and fluence of laser pulse incident on the superconductor sensor were ~ 2.7 kW / cm^2 and 10 μJ / cm^2 respectively. Under this condition, the responsivity was evaluated to be r ~ 45 V / MW when the superconductor detector was biased at T = 105 K and I = 10 mA. The transient response of the latter device is seen to exhibit a relatively slow recovery after completion of the single laser pulse. The rise time, fall time, and pulse width of this response, as shown in Table III, are many times larger than the time constants of the incident pulse. As for the previous case, these results again suggest a predominantly bolometric origin of the observed response. The absence of the nonbolometric response under the conditions of this study may be attributed to different causes. One possible cause is the large thickness (~ 240 nm) of the film sensor. In a thick film, since the recombination time of the quasiparticles is much shorter than the diffusion time, the nonbolometric signal induced within the absorption depth may be short-circuited by the superconductivity of the dark portion of the film.

In order to assess the potential of using the PbBiSrCaCuO detector as a high power detector, the surface damage threshold of the film sensor was further evaluated. Due to the difficulty in correctly comparing different microstructures of granular polycrystal films, the change in the film resistance R after an exposure to laser irradiation was instead considered as an indication of surface damage. The damage threshold value was defined to be one order of magnitude below the value of incident fluence above which R is modified. The Q-switched Nd:YLF laser whose output characteristic was given in Fig. 8 and Table III was used as radiation source in this experiment. For a 200-nm thick sensor, the surface damage threshold measured at T = 300 K was ~ 10 mJ / cm^2 per 3 ns pulse for a pulse repetition frequency of 1 kHz. This relatively large value shows that PbBiSrCaCuO sensors can inherently withstand high power laser beams being used intentionally to defeat them. Subsequent testing of the exposed detector also confirmed that exceeding the threshold only degrades detector performance without causing complete failure.

V. CONCLUSION

PbBiSrCaCuO superconductor detectors were fabricated and characterized at millimeter and infrared wavelengths. The detector unit comprises a film sensor housed in a small cryostat with built-in bias supply and temperature control circuitry. The film sensor was first deposited by magnetron rf sputtering and then crystallized under a rapid thermal annealing process which controlled its operating temperature range. The millimeter wave response exhibited a fast Josephson component with a D^* ~ 10^8 - 10^9 cm.Hz$^{1/2}$ / W in the wavelength range of 3 - 8 mm. The response to short millimeter wave pulses indicated a time constant smaller than 10 ns for this component. The infrared response did not show nonthermal components under the conditions used in this work. Preliminary studies on the bolometric response to laser pulses confirmed the potential of PbBiSrCaCuO detectors for wide band detection of high power laser beams. These studies also established that the detectors can withstand fluences exceeding 10 mJ / cm^2 for 3 ns pulses and their response to high power pulses is inherently compressible.

The above results suggest that the developed devices may be useful as primary or complementary detectors in applications which require a wide band coverage in different spectral regions. Their figure of merit has not yet been optimized, meaning that the detector performance can be substantially improved. For example, the radiation absorbance can be enhanced by integrating the detector to a broadband antenna or by coating the sensor with antireflective layers. Also, work is under way to estimate the optimum parameters of

the film sensor including film thickness, granularity, and resistivity.

ACKNOWLEDGMENT

The author wishes to thank B. Tremblay for his technical assistance.

[1] Y. Enomoto and T. Murakami, "Optical Detector Using Superconducting $BaPb_{0.7}Bi_{0.3}O_3$ Thin Films", J. Appl. Phys. 59, pp. 3807-3814 (1986).

[2] C. L. Bertin and K. Rose, "Enhanced-Mode Radiation Detection By Superconducting Films", J. Appl. Phys. 42, pp. 631-642 (1971).

[3] L. Ngo Phong, B. Tremblay, D. Côté, I. Shih, and C. X. Qiu, "Thin Film Fabrication of Pb Doped BiSrCaCuO Superconductor", in Proceedings 4th Can. Conf. on Electrical and Computer Engineering 1, edited by D. Laurendeau (IEEE/CSECE), pp. 29.4.1-29.4.4 (1991).

[4] L. Ngo Phong, B. Tremblay, I. Shih, and C. X. Qiu, "Accelerated Formation of the High-T_c Phase in Moderately Pb Doped BiSrCaCuO Thin Films", Supercond. Sci. Technol. 5, pp. 555-560 (1992).

[5] L. Ngo Phong and I. Shih, "Photoresponses of Granular (Pb)BiSrCaCuO Films to Millimeter Wavelength Radiation", J. Appl. Phys. 74, pp. 7414-7421 (1993).

[6] S. D. Peacor and C. Uher, "Thermal Conductivity of BiSrCaCuO Superconductors: Correlation with the Low-Temperature Specific-Heat Behavior", Phys. Rev. B 39, pp. 11559-11562 (1989).

[7] R. A. Fisher, S. Kim, S. E. Lacy, N. E. Phillips, D. E. Morris, A. G. Markelz, J. Y. T. Wei, D. S. Ginley, "Specific-Heat Measurements on Superconducting BiCaSrCu and TlCaBaCu Oxides: Absence of a Linear Term in the Specific Heat of BiCaSrCu Oxides", Phys. Rev. B 38, pp. 11942-11945 (1988).

[8] Semiconductors and Semimetals - Vols. 5 and 12: Infrared Detectors I and II, edited by R. K. Willardson and A. C. Beer (Academic Press, New York, 1977).

[9] L. C. Brunel, S. G. Louie, G. Martinez, S. Labdi, and H. Raffy, "Superconducting Gap in $Bi_2Sr_2CaCu_2O_8$", Phys. Rev. Lett. 66, pp. 1346-1349 (1991).